Nucleic Acids Research, 2026, **54**, gkag041
https://doi.org/10.1093/nar/gkag041
Chemical Biology and Nucleic Acid Chemistry

i-Motif, not G-quadruplex, stability regulates insulin expression

Dilek Guneri [1,2], Christopher J Morris [1], Yiliang Ding [3,*], Timothy D Craggs [4,*], Steven S Smith [5,*], Zoë AE Waller [1,*]

[1]School of Pharmacy, University College London, 29-39 Brunswick Square, London WC1N 1AX, United Kingdom
[2]School of Health, Science and Society, University of Suffolk, 19 Neptune Quay, Ipswich IP4 1QJ, United Kingdom
[3]Department of Cell and Developmental Biology, John Innes Centre, Norwich Research Park, Norwich NR4 7UH, United Kingdom
[4]Department of Chemistry, University of Sheffield, Western Bank, Sheffield, United Kingdom
[5]Department of Stem Cell Biology and Regenerative Medicine, Beckman Research Institute of the City of Hope, 1500 E. Duarte Road, Duarte CA 91010-3000, United States

*To whom correspondence should be addressed. Email: z.waller@ucl.ac.uk
Correspondence may also be addressed to Steven S. Smith. Email: SSmith@coh.org
Correspondence may also be addressed to Yiliang Ding. Email: Yiliang.Ding@jic.ac.uk
Correspondence may also be addressed to Timothy D. Craggs. Email: t.craggs@sheffield.ac.uk

Abstract

The insulin-linked polymorphic region (ILPR) is a variable number tandem repeat located in the promoter of the human insulin gene. This G-rich sequence can fold into four-stranded G-quadruplex DNA structures, while its complementary C-rich strand forms i-motifs. The ILPR varies in repeat number and sequence composition, but the relationship between sequence diversity, DNA structure, and insulin gene regulation remains poorly understood. Although both G-quadruplexes and i-motifs have been implicated in transcriptional control, their relative contributions, particularly when formed on complementary strands of the same locus, are unclear. Here, we characterized the structure and stability of nine ILPR-based sequences using biophysical techniques and luciferase reporter assays. We demonstrate that transcriptional activation in response to high glucose occurs only when both G-quadruplex and i-motif structures can form. Other combinations of structures do not induce transcription. Moreover, promoter activity correlated positively with i-motif stability, but not with G-quadruplex stability. These results suggest a model in which G-quadruplexes may act as an initiation site, while i-motifs act as modulators of insulin gene expression. Our findings underscore the importance of treating G-quadruplexes and i-motifs as a dynamic, interdependent system in both the regulation of gene expression and also the potential of these structures as therapeutic targets.

Graphical abstract

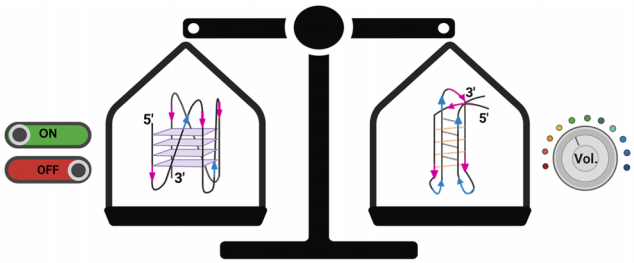

Introduction

Insulin is a central protein hormone regulating glucose metabolism. Deficiencies of insulin production can cause hyperglycaemia and lead to diabetes mellitus [1, 2]. The insulin-linked polymorphic region (ILPR) is found 363 bp upstream of the human insulin transcription start site [3–5]. This heterogeneous region may vary in nucleotide composition and the number of tandemly repeated ILPR sequences among individuals [2, 5–8]. A shortened ILPR repeat length is linked with Type-1 Diabetes [1] while some variations in the sequence composition are linked to Type-2 Diabetes [2, 5, 7–10]. The ILPR is found to regulate insulin as well as insulin-like growth factor 2 and small variations in the ILPR sequence are associated with decreased gene expression in both genes [7, 11, 12].

The ILPR comprises a variable number of tandem repeats with sequence variability, the predominant sequence being 5′-ACAGGGGTGTGGGG-3′/3′-TGTCCCCACACCCC-5′ [5, 7, 8], This GC-rich DNA region has the potential to form non-canonical DNA structures. The C-rich sequence can fold into i-motif structures that are stabilized by pH, negative supercoiling, and molecular crowding [13–17]. The complementary

Received: May 2, 2025. **Revised:** December 6, 2025. **Accepted:** December 28, 2025

G-rich sequence is arranged as planar G-quartets held together by Hoogsteen hydrogen-bonding and stabilized via π–π stacking and cations [18–20]. These types of noncanonical DNA structures have been shown, in cells, to be prevalent in the promotor regions of genes and to appear at certain cellular events [5, 21–24]. Recently, we characterized 11 of the most common native ILPR variants and established a relationship between i-motif and G-quadruplex structure formation regulating reporter gene expression in cultured INS-1 cells [25]. This then led to the question of which is more important for insulin expression: G-quadruplex or i-motif structure?

Early research showed that ILPR variants influence Pur-1-mediated gene expression, with the predominant sequence eliciting the strongest response, speculatively due to the formation of inter- and intramolecular G-quadruplex structures [8]. Chemical foot-printing and mechanical folding experiments *in vitro* have indicated that both G-quadruplex and i-motif structures may form within the double-stranded ILPR region, but the structures are indicated to be mutually exclusive [26]. However, more recently, we were able to demonstrate a link between the noncanonical DNA structure formation and regulation of gene expression [25]. Based on the biophysical data and biological experiments, we sought to determine which structure plays a more important role in regulating insulin reporter expression.

Herein, we determine a precise relationship between noncanonical DNA structure formation and stability, and the expression of the ILPR-regulated reporter gene. Through a systematic study of mutant ILPR sequences we show that both G-quadruplex and i-motif are essential for insulin reporter expression and the level of expression correlates positively with i-motif, but not G-quadruplex, stability.

Materials and methods

Oligonucleotides

All synthetic oligonucleotide sequences used in this study were synthesized and reverse-phase HPLC purified by Eurogentec (Belgium). Samples were prepared at a final concentration of 1 mM in ultra-pure water and concentrations were confirmed using a Nanodrop spectrophotometer. For DNA structure annealing, samples in buffer, as specified in experimental sections, were heated at 95°C for 5 min in a heating block, followed by slow cooling to room temperature overnight.

Circular dichroism spectroscopy

Circular dichroism (CD) spectra of the selected ILPR sequences were recorded using a JASCO J-1500 spectropolarimeter under a constant flow of nitrogen. C-rich ILPR samples were diluted to 10 μM in 10 mM sodium cacodylate buffer (NaCaco, Merck) containing 100 mM KCl, and measured across a pH range of 4–8. G-rich ILPR samples were prepared at 10 μM in 10 mM NaCaco with either 100 mM KCl, 100 mM NaCl, or 100 mM LiCl at pH 7.0 to assess cation-specific folding. For each buffer and sample, four spectra scans were accumulated over a range of 200–320 nm at 20°C, using a data pitch of 0.5 nm, scanning speed of 200 nm/min, 1-s response time, 1 nm bandwidth, and a sensitivity setting of 200 mdeg. Spectra were baseline-corrected at 320 nm. The transitional pH (pH_T) of the C-rich ILPR sequences was determined from triplicate experiments by fitting a sigmoidal curve to the ellipticity at 288 nm across the pH range, with the inflection point representing the pH_T.

Ultraviolet melting/annealing and TDS

Ultraviolet (UV) melting/annealing and TDS experiments were carried out using a Jasco V-750 UV–Vis spectrophotometer. C-rich ILPR samples were prepared at 2.5 μM in 10 mM NaCaco buffer with 100 mM KCl at pH 5.5, while G-rich ILPR samples were annealed at 2.5 μM in 10 mM NaCaco with 20 mM KCl at pH 7.0. Samples were initially held at 4°C for 10 min, then subjected to three thermal cycles of melting and annealing. During melting, the temperature was gradually increased from 4°C to 95°C at a rate of 0.5°C/min, with absorbance recorded at 260 and 295 nm in 1°C intervals, following a 5-min hold at each temperature. After a 10-min hold at 95°C, the process was reversed for annealing.

Absorbance values were baseline-corrected, and the fraction folded was calculated for both wavelengths. The melting temperature (T_m) and annealing temperature (T_a) were determined using the first derivative of the corrected and normalized data for each cycle [27].

For TDS analysis, spectra were recorded between and 320 nm after maintaining the samples at 4°C (folded) and 95°C (unfolded) for 10 min each. The TDS profile was generated by subtracting the folded spectrum from the unfolded spectrum, zero-corrected at 320 nm, and normalized to the maximum absorbance to reveal structure-specific signatures.

Cell culture

INS-1 rat insulinoma cells (AddexBio, Catalogue No. C0018007) were cultured in RPMI-1640 medium supplemented with 10% fetal bovine serum, 50 μM 2-mercaptoethanol, and 1% penicillin–streptomycin (all reagents from Gibco). Cells were maintained at 37°C in a humidified incubator with 5% CO_2. The culture medium was replaced every three days, and cells were passaged upon reaching ∼80% confluency. All experiments were performed using cells between passages 10 and 14.

Transfection of reporter gene plasmids

The firefly luciferase reporter gene was placed under the control of a modified human insulin promoter containing 2.5 repeats of ILPR variant segment or corresponding mutant segments. INS-1 cells were co-transfected with the pRL-TK Renilla reference vector under previously described conditions [25]. For data analysis, we adapted the approach described by Baker and Boyce to calculate the promoter induction ratio [28]. Specifically, each Firefly:Renilla ratio was normalized by dividing it by the average Firefly:Renilla ratio of the corresponding plate, excluding the top and bottom 25% of wells to minimize the influence of outliers. This refinement enabled a more accurate distinction between the transcriptional activities of different ILPR variants and mutants in response to either 2.or 16.2 mM glucose stimulation.

Results and discussion

Selection of ILPR variant sequences for analysis

We designed systematic mutations within the cytosine tract or the loop region of the C-rich ILPR variants, generating a biophysical landscape for a wide range of i-motif stabil-

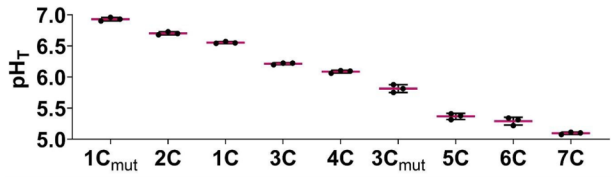

Figure 1. Highest to lowest transitional pH (pH$_T$) of selected C-rich ILPR variants including mutants as determined by CD spectroscopy. Data shown as mean ± standard deviation (SD; $n = 3$). Source data are available.

ities (Supplementary Table S1) [25, 29]. From this library, we selected nine ILPR sequences, comprising seven naturally-occurring native variants and two systematically modified mutants (1C$_{mut}$, 2C, 1C, 3C, 4C, 3C$_{mut}$, 5C, 6C, and 7C). For clarity, we refer to the naturally derived sequences as ILPR variants, and to the artificially introduced sequence modifications as ILPR mutants. The transitional pH (pH$_T$) was determined from CD spectra recorded across a range of pH values and represents the pH at which 50% of the i-motif population is folded/unfolded. This value serves as a quantitative indicator of i-motif stability [13, 16, 30, 31]. We aimed for a broad range of transitional pHs to enable determination of a potential cut-off point in i-motif stability that may affect gene expression and selected nine variants for further evaluation (Fig. 1). The selected G/C-rich ILPR sequences are summarized in Table 1 (C-rich variants) and Table 2 (G-rich variants).

Effects of non-native mutations on ILPR variant sequence topologies

Mutations in the loop regions of the prevalent ILPR sequence 1C (from an ACA loop to a TCT) was found to further stabilize the i-motif from pH$_T$ 6.6 to pH$_T$ 6.9 (Table 1 and Supplementary Fig. S1A/F and B/G, P <.0001). This is consistent with other studies that indicated that having TT base pairs in the loops provides additional stability [25, 32]. For example, a DNA microarray of 10 976 potential i-motif–forming sequences revealed that i-motifs with short loops (1–4 nucleotides) were more stable when thymine residues flanked the cytosine tracts [32]. We have also observed TT base pairs in the ILPR structure through the crystal structure, nuclear magnetic resonance (NMR) experiments, and supporting molecular dynamics simulations of the ILPR i-motif [25]. TT base pairs have previously been shown to stabilize noncanonical DNA structures by forming reverse Hoogsteen hydrogen bonds or loop-stabilising interactions, particularly under mildly acidic or dehydrated conditions, contributing to structural integrity and pH responsiveness in i-motifs and triplexes [33]. The mutation in the loop of ILPR 3C (from AGA to AGG) decreased the transitional pH from 6.2 to 5.8 (Table 1 and Supplementary Fig. S1D/I and E/J, P <.0001). This is consistent with findings by Benabou *et al*., which indicated that the incorporation of guanine bases into the loops of an i-motif decrease i-motif stability while thymine or cytosine residues in these positions enhance i-motif stability [34]. Seven out of the nine selected C-rich ILPR variants were found to fold into i-motifs with pH$_T$-values between pH 5.4 and 6.9 and these unfold into a what appears to be a random coil. CD spectroscopy of ILPR 1, ILPR 1C$_{mut}$, ILPR 2C, ILPR 3C$_{mut}$, ILPR 4C, and ILPR 5C showed i-motif formation at acidic pH, indicated by a positive peak at 288 nm and a negative peak at 260 nm, and as the pH increases the structure unfolds, shifting the positive peak between 275 and 280 nm and the negative peak to 240 nm (Supplementary Figs S1 and S2). Typical i-motif spectra have been shown to shift their positive bands from about 288 to 280 nm [35–37]. However, ILPR 6C and ILPR 7C have a positive peak at 285 nm which shifts to about 283 nm (Fig. 1, Table 1, and Supplementary Fig. S2C/G and D/H), indicating the formation of hairpins [38, 39]. UV melting/annealing experiments are widely used to determine the thermal stability [27, 40]. We expanded on the range of thermal stability profiles for the native C-rich ILPR variants [25], with the two mutant sequences (Supplementary Fig. S3). The ILPR 1C$_{mut}$ showed an increased thermal stability compared to the predominant ILPR 1C variant (Supplementary Table S1, P <.0001). However, ILPR 3C$_{mut}$ has comparable thermal stability to ILPR 3C (Table 1 and Supplementary Fig. S3, P = 0.07).

Thermal difference spectroscopy (TDS) is commonly used to identify secondary DNA structures in solution, providing distinct spectral profiles that reflect on structural features. Both mutant ILPR sequences displayed TDS signatures with positive peaks at 240 and 265 nm and a negative peak at 295 nm (Supplementary Fig. S4), consistent with the presence of i-motif structures [41]. However, ILPR 6C presents as an intriguing candidate, exhibiting features of a hairpin in both CD spectra and TDS profile at pH 5.5, yet displaying a distinct melting profile in UV absorbance at 295 nm, an unusual characteristic for canonical hairpin structures. This suggests the presence of a minor population of noncanonical DNA conformations, such as i-motifs or triplexes, which are known to exhibit melting profiles at 295 nm due to base stacking interactions and structural transitions specific to these motifs [42].

The complementary native G-rich ILPR sequences have been previously studied [12, 43–47]. One study identified a correlation between G-quadruplex conformation and selective binding affinity of insulin and insulin-like growth factor [47]. We previously reported the biophysical characterization of the G-rich ILPR sequences showing that only 3 of the native 11 ILPR sequences in the human insulin promotor element form stable G-quadruplexes, here renamed to 1G, 2G, and 3G [25]. We sought to determine whether the shifts in pH$_T$ that were associated with mutations in loops of the 1C and 3C sequences were mirrored by changes in the complementary mutant G rich strand i.e. 1G$_{mut}$ and ILPR 3G$_{mut}$. We used QGRS mapper [48] to predict the stability of both mutant ILPR G-rich mutants, which exhibited a QGRS score of 63 as 1G, 2G, and 3G (Table 2).

The G-rich ILPR sequence variants were characterized by CD spectroscopy in 10 mM Na cacodylate buffer (pH 7.0) containing 100 mM KCl, NaCl, or LiCl, to assess cation preferences, commonly used to observe cation dependent G-quadruplex topologies. Interestingly, the CD spectrum of ILPR 1C$_{mut}$ has the typical profile for a parallel G-quadruplex with a positive peak at 264 nm and a negative peak around 240 nm (Supplementary Fig. S5A). However, ILPR C1 is a mixed population of parallel and antiparallel G-quadruplexes, presenting with a negative peak at 240 nm, and positive peaks at 263 and 295 nm (Supplementary Fig. S5B). In potassium chloride, ILPR 3G$_{mut}$ exhibits a mixed population with a higher tendency towards parallel G-quadruplex topology than antiparallel G-quadruplex topology, while in sodium chloride and lithium chloride the mixed topology has a higher preference for antiparallel G-quadruplex topology over

Table 1. Biophysical characterization via CD spectrum, UV melt and anneal, and thermal difference spectrum of C-rich ILPR mutants in comparison with naturally occurring ILPR variants as published in Guneri *et al.* (2024)

		UV spectroscopyMelting, annealing temperatures (°C)					
		295 nm		260 nm		CD	TDS
ILPR	Sequence	T_M	T_A	T_M	T_A	pH_T	structure
$1C_{mut}$	TGTCCCCTCTCCCCTGTCCCCTCTCCCCTGT	60 ± 0.6	57 ± 0.6	61 ± 0.6	58 ± 0.6	6.9	iM
1C	TGTCCCCACACCCCTGTCCCCACACCCCTGT	55 ± 0.2	53 ± 0.6	56 ± 0.0	53 ± 0.6	6.6	iM
2C	TATCCCCACACCCCTATCCCCACACCCCTAT	57 ± 0.6	54 ± 0.0	57 ± 0.5	54 ± 0.0	6.7	iM
3C	TGTCCCCAGACCCCTGTCCCCAGACCCCTGT	50 ± 0.0	48 ± 0.0	50 ± 0.6	48 ± 0.0	6.2	iM
4C	TGTCCTCACACCCCTGTCCTCACACCCCTGT	40 ± 0.6	37 ± 0.5	40 ± 0.6	37 ± 0.5	6.1	iM
$3C_{mut}$	TGTCCCCAGGCCCCTGTCCCCAGGCCCCTGT	52 ± 1.0	47 ± 0.1	52 ± 0.6	47 ± 0.3	5.8	iM
5C	TGTCCTCAGACCCCTGTCCTCAGACCCCTGT	32 ± 0.0	28 ± 0.6	32 ± 0.0	29 ± 0.6	5.4	iM
6C	TGTGCCCACACCCCTGTGCCCACACCCCTGT	50 ± 0.6	44 ± 0.6	50 ± 0.7	44 ± 0.0	5.2	Hp
7C	TGTCCCCAGGACCCTGTCCCCAGGACCCTGT	–	–	60 ± 0.6	57 ± 0.0	5.1	Hp

–, not detected; T_M, Melting temperature; T_A, Annealing temperature; pH_T, Transitional pH; iM, i-Motif; Hp, Hairpin.

Table 2. Biophysical characterization via CD spectrum, UV melt and anneal, thermal difference spectrum, and QGRS mapper score of G-rich ILPR mutants in comparison with naturally occurring ILPR variants as published in Guneri *et al.* (2024)

		UV spectroscopyMelting, annealing temperatures (°C)						
		295 nm		260 nm		CD	TDS	
ILPR	Sequence	T_M	T_A	T_M	T_A	structure		QGRS score
$1G_{mut}$	ACAGGGGAGAGGGGACAGGGGAGAGGGGACA	82 ± 0.6	72 ± 1.0	83 ± 0.6	72 ± 0.7	G4	G4	63
1G	ACAGGGGTGTGGGGACAGGGGTGTGGGGACA	76 ± 0.6	60 ± 0.0	77 ± 0.6	60 ± 0.6	G4	G4	63
2G	ATAGGGGTGTGGGGATAGGGGTGTGGGGATA	79 ± 0.6	60 ± 0.6	79 ± 0.6	60 ± 0.6	G4	G4	63
3G	ACAGGGGTCTGGGGACAGGGGTCTGGGGACA	82 ± 0.7	56 ± 0.6	81 ± 0.6	57 ± 0.7	G4	G4	63
4G	ACAGGGGTGTGAGGACAGGGGTGTGAGGACA	30 ± 0.0	27 ± 0.6	31 ± 0.6	28 ± 0.6	Hp	Hp	21
$3G_{mut}$	ACAGGGGCCTGGGGACAGGGGCCTGGGGACA	74 ± 0.6	60 ± 0.0	75 ± 0.6	60 ± 0.7	G4	G4	63
5G	ACAGGGGTCTGAGGACAGGGGTCTGAGGACA	–	–	51 ± 0.0	48 ± 0.6	Hp	Hp	21
6G	ACAGGGGTGTGGGCACAGGGGTGTGGGCACA	56 ± 0.0	50 ± 0.0	56 ± 0.6	51 ± 0.6	Mix	Mix	42
7G	ACAGGGTCCTGGGGACAGGGTCCTGGGGACA	–	–	57 ± 0.6	51 ± 0.6	Hp	Hp	42

–, not detected; GQRS score, Quadruplex forming G-rich sequences score; T_M, Melting temperature; = T_A, Annealing temperature; pH_T, Transitional pH; G4, G-quadruplex; Hp, Hairpin; Mix, mixture of G4 and Hp.

parallel G-quadruplex topology (Supplementary Fig. S5E). These structural preferences in the three tested cations were reversed for the ILPR 3G variant. UV-melt analysis of $1G_{mut}$ shows a significantly increased melting and annealing temperature (Supplementary Fig. S6) compared to the native ILPR 1G variant (Table 2, $P > .001$). ILPR $3G_{mut}$ has a significantly lower melting and anneal temperature compared to the native ILPR 3G variant (Table 2, $P > .001$) [25]. The thermal difference spectrum provides profiles of typical G-quadruplex formation for both tested G-rich ILPR mutant sequences (Supplementary Fig. S7) [41].

Glucose and glucose-6-phosphate affect the stability and structure of some ILPR variants *in vitro*

When glucose enters an insulin-secreting cell, the normal response of the insulin gene is induction of insulin expression. It is already known that as glucose enters a cell the pH decreases [49] and the concentration of potassium increases [50]. These conditions will inherently stabilize formation of both i-motif and G-quadruplex structures. However, it is not clear whether glucose itself affects the stability or conformation of these structures directly. With this in mind, we investigated the effects of glucose on ILPR variants 1C/G, which form i-motif/G-quadruplex structures and 6C/G which form a hairpin/mixture of structures. After entering the cell, glucose quickly metabolizes to glucose-6-phosphate (G6P) [51] which can diffuse through nuclear pores and is thought to reach nucleoplasmic concentrations comparable to levels in the cytoplasm [52–55], thought to be in the tens to hundreds of micromolar range [56], but there is uncertainty around the exact concentration. Accepting this is unknown, we decided to examine the effects of glucose and G6P on ILPR oligonucleotides at 2.8 mM and 16.2 mM, to match the conditions used in our previous reporter gene assays [25]. We performed TDS and UV melting. Results can be found in Supplementary Table S2 and Supplementary Figs S8 and S9).

TDS analyses revealed distinct and sequence-dependent effects of glucose and G6P on ILPR conformational equilibria. For the i-motif-forming ILPR 1C, the characteristic TDS signature was preserved in the presence of glucose (Supplementary Fig. S8A). In contrast, 16.2 mM G6P profoundly altered the spectrum, producing a strong positive peak at 260 nm and a diminished negative peak at 295 nm, indicative of a shift in conformation with only minor contributions from residual i-motif. These findings demonstrate that high G6P concentrations can destabilize the ILPR 1C i-motif. The hairpin-forming ILPR C6 exhibited pronounced environmental sensitivity. At low glucose (2.8 mM), the TDS profile showed partial i-motif character, which became more distinct at 16.2 mM glucose, suggesting glucose may promote fold-

ing of this sequence into an i-motif (Supplementary Fig. S8B). In contrast, G6P induced progressive unfolding: 2.8 mM G6P reduced the i-motif-like contribution, and 16.2 mM G6P abolished the 295 nm feature entirely. These data show that ILPR C6, though initially classified as a hairpin in our standard buffer conditions, has the intrinsic structural plasticity to form an i-motif under high glucose, but is destabilized in the presence of high G6P, where only a hairpin remains. For G-rich ILPR variants, TDS signatures were generally more robust. ILPR G1 retained canonical G-quadruplex profiles in all conditions (Supplementary Fig. S8C). ILPR G6, which adopts mixed G-quadruplex/hairpin conformations, shifted toward a more pronounced G-quadruplex signature in the presence of glucose, whereas G6P induced a mixed but increasingly G-quadruplex-favoured population (Supplementary Fig. S8D). UV-melting experiments complemented the TDS results by quantifying the thermodynamic stability of each structural state. For ILPR 1C, melting temperatures were unchanged in the presence of glucose but decreased progressively with increasing G6P concentration, falling from 55°C to 42°C (2.8 mM G6P) and 34°C (16.2 mM G6P). ILPR 6C displayed two distinct melting transitions in low glucose, consistent with coexisting structural populations, whereas high glucose yielded a single transition with a higher T_M (68°C), supportive of stabilization of a single structure, which the TDS indicates would be an i-motif. G6P reduced stability in a concentration-dependent manner, and at 16.2 mM G6P, the UV melting was poorly defined at 295 nm, indicating a shift towards a lower-stability hairpin. ILPR 1G exhibited an additional high-temperature transition (84°C) in glucose, suggesting the emergence of a highly stable G-quadruplex population. In ILPR 6G, the experiments in the presence of glucose produced two melting transitions and shifted equilibria between structural states, whereas G6P resulted in a single transition around ∼70°C at both wavelengths, again consistent with the TDS-observed structural consolidation to one G-quadruplex, rather than a mix of G-quadruplex and hairpin structures.

Collectively, these biophysical measurements reveal that glucose and G6P do not uniformly stabilize or destabilize ILPR structures but have nuanced, sequence-dependent effects that modulate conformational equilibria *in vitro*. In particular, the mixed/hairpin-forming sequences (C6, G6) seem highly responsive to environmental perturbation. Importantly, G6P at high concentrations disrupts i-motif stability more than glucose, suggesting that phosphorylated glucose metabolites, but not glucose itself, may have the capacity to modulate non-canonical DNA structures directly, in addition to the cellular changes in intracellular pH and cationic conditions that can influence DNA structures [49, 50]. Although the nuclear concentrations of glucose and G6P remain unknown, our findings provide a conceptual framework linking cellular metabolic state to the structural dynamics of noncanonical DNA elements within the insulin promoter. The biophysical data together indicate that ILPR sequences span a continuum from rigid, high-stability i-motifs/G-quadruplexes to highly adaptive hairpin-capable elements sensitive to local physicochemical conditions. This suggests a potential mechanism by which fluctuations in intracellular glucose metabolism, particularly shifts in G6P availability, could influence regulatory DNA architecture and thereby contribute to transcriptional modulation of the insulin gene. While speculative, this model aligns with emerging evidence that nuclear metabolism can impact chromatin function and gene regulation.

Both G-quadruplex and i-motif structures are required for reporter gene transcription

To further investigate the hypothesis that i-motifs and G-quadruplexes formed within the ILPR act as regulatory elements capable of modulating insulin transcription, we selected naturally occurring ILPR variants and ILPR mutant sequences that adopted distinct combinations of DNA secondary structures in biophysical experiments: G-quadruplex and i-motif; hairpin and hairpin; and i-motif and hairpin. Despite examining over 50 ILPR-like sequences, we did not identify any combinations in which the formation of G-quadruplex structure was accompanied by a C-rich hairpin in the complementary strand (Supplementary Table S1). Instead, C-rich sequences forming hairpins were typically paired with G-rich hairpins rather than G-quadruplexes. We speculate that G-quadruplexes may be more prone to disruption by sequence mutations, which is also supported by previous studies showing that even single nucleotide substitutions within G-rich regions, such as those in the c-MYC promoter, can destabilize G-quadruplex formation and shift the structural equilibrium toward alternative conformations, including hairpins [57–59]. We hypothesize that the sequence requirements for a G-quadruplex to form are more stringent than that for formation of an i-motif structure, so if there are enough guanines to form a G-quadruplex, there will always be enough complementary cytosines to form an i-motif. The nine characterized ILPR sequences were cloned upstream of the human insulin promoter to regulate firefly luciferase expression in reporter gene assays, where luciferase activity serves as a proxy for promoter activation. Insulin-secreting β-cells respond to elevated glucose levels, enabling the assessment of ILPR-mediated regulation under physiologically relevant conditions linked to glucose homeostasis [60]. The rat insulinoma-derived cell line INS-1, widely used to study β-cell function, lacks an intrinsic ILPR or any known homologous sequence, making it a suitable model system for dissecting ILPR-mediated transcriptional regulation [25, 61, 62]. INS-1 cells were co-transfected with ILPR–luciferase constructs and a Renilla luciferase plasmid to normalize transfection efficiency. Following overnight serum and glucose starvation, the cells were exposed to either low (2.8 mM) or high (16.2 mM) glucose for 4 h to assess glucose-responsive transcriptional activity, consistent with established protocols [25, 63–65]. We tested three categories of ILPR-regulated firefly reporter vectors: those forming G-quadruplexes and i-motifs (ILPR 1, 1_{mut}, 2, 3, and 3_{mut}), those forming hairpins on both DNA strands (ILPR 6 and 7), and those forming an i-motif and a hairpin (ILPR 4 and 5).

Under low glucose conditions (2.8 mM), ILPR 1_{mut} showed a significantly increased firefly luciferase activity compared to ILPR 1 (Fig. 2, P <.001). In contrast, reporter constructs driven by ILPRs 2, 3, 4, 3_{mut}, 4, and 5 showed no significant differences in expression levels relative to ILPR 1 (P >.24), while ILPR 6 and 7 exhibited significantly reduced firefly activity (P <.001). At high glucose concentrations (16.2 mM), ILPR 1_{mut} again displayed significantly increased expression compared to ILPR 1 (P <.001). Meanwhile, ILPR 2 (P = 0.005), ILPR 3, and ILPR 3_{mut} demonstrated significantly decreased firefly activity (P <.001). No significant changes were observed for ILPR 4, ILPR 5, ILPR 6, or ILPR 7 under high glucose conditions. Interestingly, reporter constructs driven by ILPR sequences known to form i-motif and G-quadruplex structures *in vitro* (ILPR 1, ILPR 1_{mut}, ILPR 2, ILPR 3, and ILPR 3_{mut}) showed a significant overall increase

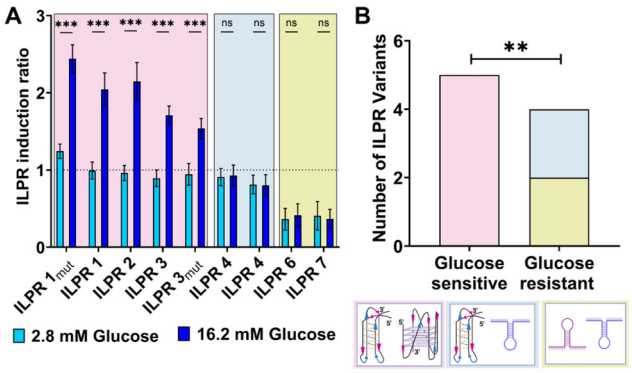

Figure 2. Dual Luciferase reporter gene assay in co-transfected INS-1 cells to determine response to 2.8 mM glucose (bright blue) and 16.2 mM glucose (dark blue) of firefly luciferase regulated by i-motif/G-quadruplex (pink background), hairpin/hairpin (blue background), and iM/hairpin (gold background) forming ILPR variants (**A**). Mean ± standard error of the mean (seven biological repeats each with three technical repeats); two-way Analysis of Variance (ANOVA) with Holm–Šidák *post hoc* corrections; $P < .001^{***}$, ns > .1. Fisher's exact test displays a significant association ($P = 0.008$) between G4/iM formation and glucose response in comparison to variants incapable to form both higher order noncanonical structures that remain nonresponsive to glucose levels in cell-based reporter gene expression assay (**B**).

in firefly luciferase activity when glucose levels were high (16.2 mM) compared to low glucose conditions ($P < .001$). The findings for ILPR 1, ILPR 2, ILPR 4, and ILPR 5 are consistent with our previous study [25] where we observed that sequences which form both G-quadruplexes and i-motifs in *in vitro*, showed increased firefly reporter gene expression in transfected INS-1 cells when treated with high glucose. In contrast, sequences, which form hairpins on both strands, showed no significant changes in expression between low and high glucose conditions.

Plasmids containing ILPR 1, ILPR 1_{mut}, ILPR 2, ILPR 3, and ILPR 3_{mut} showed significantly increased firefly gene expression in response to high glucose levels compared to low glucose conditions ($P < .001$). All five ILPR variants share underlying sequences capable of forming both i-motif and G-quadruplex structures and responded to glucose level changes in a similar manner. However, the increase in expression was significantly greater for ILPR 1_{mut}, which also exhibited the most stable noncanonical DNA structures in the biophysical characterization ($P < .001$). Importantly, reporter constructs containing ILPR sequences that do not form i-motif or G-quadruplex structures (ILPR 6 and 7) showed no changes in firefly gene expression under high glucose conditions ($P > .99$). Similarly, ILPR 4 and ILPR 5, which are associated with sequences which form weak i-motif and complementary G-rich hairpin structures *in vitro*, also showed no significant changes in response to glucose level variation ($P > .99$), indicative that this combination of structures does not trigger expression. These data highlight the potential significance of sequence variation within the ILPR, suggesting that the distinct DNA structures formed—such as i-motifs, G-quadruplexes, and hairpins—may influence the responsiveness to glucose. The findings suggest that even minor sequence alterations can result in substantial differences in both the formation and stability of DNA secondary structures, underlining the regulatory importance of both i-motif and G-quadruplex structures in controlling reporter gene expression.

Next, we interrogated whether glucose responsiveness was significantly associated with structural features of the ILPR sequences. Specifically, we compared glucose-sensitive and glucose-resistant ILPRs across three structural categories: (i) i-motif and G-quadruplex forming sequences, (ii) hairpins on both strands, and (iii) i-motif and G-rich hairpin combinations regulating firefly reporter gene expression. To assess the association between glucose responsiveness and the ability to form i-motif/G-quadruplex (i-motif/G-quadruplex) structures, we applied a Fisher's exact test (Fig. 2B). Fisher's exact test was chosen because it is particularly well-suited for small sample sizes and categorical data, such as the binary classification of ILPR variants into glucose-responsive versus nonresponsive, and i-motif/G-quadruplex-forming versus nonforming groups. Unlike chi-square tests, Fisher's exact test does not rely on large sample assumptions and provides an exact *P*-value, making it the most reliable option for detecting statistically significant associations in our dataset [66]. The analysis revealed a significant association between glucose responsiveness and the ability of ILPR sequences to form i-motif and G-quadruplex structures ($P = 0.008$).

i-Motif stability modulates transcriptional activity

To better understand the contribution of DNA structures to the regulation of gene expression, we aimed to determine whether i-motifs or G-quadruplexes play a more prominent role in modulating ILPR-driven promoter activity in response to glucose. We performed correlation analyses between biophysical parameters of structural stability and reporter gene expression under both low and high glucose conditions. Pearson's correlation coefficient (r) was chosen as the statistical test to assess the linear relationships between, normally distributed variables [67]. The i-motif sequences were initially characterized using transitional pH (Supplementary Fig. S1 and S2), which reflects the pH at which the C-rich strand folds into an i-motif and provides insight into its physiological relevance [13]. To enable direct comparison between i-motif and G-quadruplex forming sequences, we subsequently measured the melting temperature (T_M), which reflects the thermal stability of the folded structure. While transitional pH and T_M measure distinct aspects of the stability, they are interconnected: changes in the pH can affect both the folding state and the thermal stability of i-motifs [68, 69]. In this case here, we use T_M as a biophysical parameter to allow direct comparison with the G-quadruplex stability and to correlate these structural properties with firefly gene expression levels expressed as transcription induction ratio. This test allows us to evaluate whether increases in structural stability correlate with increased reporter activity across different ILPR variants.

Pearson's correlation analysis revealed a statistically significant positive correlation between i-motif stability, expressed as T_M, and reporter gene expression under both low (Fig. 3A, $P < .001$) and high glucose treatment (Fig. 3B, $P < .001$). This is in line with i-motif stability expressed as transitional pH (Supplementary Fig. S10), and ILPR-regulated firefly gene expression at both low (2.8 mM) and high (16.2 mM) glucose levels (Supplementary Fig. S10A, $P = .03$; Supplementary Fig. S10B, $P = .01$). The melting temperature and the transitional pH show a clear positive correlation between i-motif stability and reporter gene expression

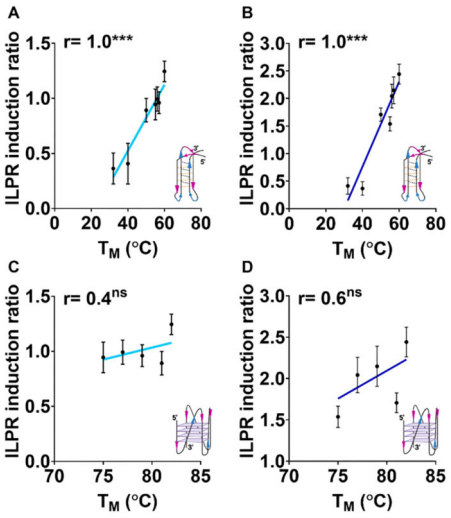

Figure 3. Pearson's correlation between melting temperature C-rich ILPR variants capable of forming i-motifs and melting temperature of G-rich variants capable G-quadruplex folding and corresponding ILPR induction ratio in dual luciferase reporter gene assay in presence of 2.8 mM glucose (**A**, **C**) and 16.2 mM glucose (**B**, **D**). Data shown as mean ± SD ($n = 6$ for reporter gene assay, $n = 3$ for biophysical data), Student's *t*-test; ns > .1, $P < .001$***.

regulated by i-motif forming ILPR sequences. In contrast, no significant correlation was found between G-quadruplex stability, as measured by melting temperature and ILPR-induced gene expression at low (Fig. 3C, $P = .31$) nor high glucose (Fig. 3D, $P = .24$) levels. These findings suggest that i-motif stability is associated with promoter responsiveness in this context, highlighting its potential regulatory relevance over G-quadruplexes in glucose-sensitive transcriptional control.

Our findings support the idea that seemingly small sequence alterations within ILPR sequences can significantly impact the formation and stability of noncanonical DNA structures, thereby modulating glucose-responsive gene expression. Notably, ILPR 1_{mut} exhibited a stronger transcriptional response and greater structural stability of i-motif and G-quadruplex formations compared to wild-type ILPR 1, suggesting that even subtle sequence changes can shift the structural equilibrium toward conformations with enhanced regulatory capacity. This observation is consistent with previous studies showing that single-nucleotide variations or loop modifications in G-rich regions of the human telomeric, Bcl-2, and c-Myc promoter sequences can disrupt G-quadruplex formation and instead favour alternative structures such as hairpins, depending on sequence context and ionic conditions [39, 59, 70]. These findings reinforce our interpretation that the differences in glucose responsiveness observed between ILPR 1 and 1_{mut}, as well as between ILPR 3 and 3_{mut}, may be attributed not only to changes in structural stability but also to a potential shift toward parallel G-quadruplex conformations, which may be more transcriptionally active [71–73]. In contrast, variants such as ILPR 4, ILPR 5, ILPR 6, and ILPR 7, which predominantly adopted hairpin-like structures, showed minimal or no transcriptional activation in response to elevated glucose. Our data thus align with and extend prior reports by demonstrating that structural shifts, driven by minor sequence changes—can have a profound functional impact in the context of glucose regulation.

On the complementary C-rich strand, our data show that mutations in ILPR variants can alter i-motif stability, but i-motif formation is less frequently disrupted compared to the G-quadruplex. This suggests that i-motifs may possess greater sequence tolerance, maintaining folded structures even in the presence of point mutations. For instance, ILPR 1_{mut} exhibited an increased transitional pH and melting temperature compared to ILPR 1, indicating enhanced i-motif stability, which positively correlated with higher reporter gene expression under both low and high glucose conditions (Fig. 3A and B). This supports the hypothesis that the structural integrity of i-motifs directly contributes to transcriptional responsiveness. Previous studies have similarly shown that single-base changes or loop bulges in i-motif-forming sequences can subtly modulate folding stability without fully abolishing structure formation. In the Bcl-2 and c-MYC promoters, for example, mutations created bulged loops or altered loop length and position, leading to changes in folding kinetics and pH responsiveness without completely preventing i-motif formation [39, 74]. Kaiser *et al.* investigated the KRAS promoter region and identified that the C-rich mid-region forms a dynamic equilibrium between i-motif, hairpin, and hybrid structures. Their study demonstrated that these structural forms are influenced by pH and that the i-motif structure can interact with the transcription factor hnRNP K to modulate KRAS transcription [75]. This suggests that structural variations, including bulges within the i-motif, can impact folding kinetics and transcriptional regulation. These findings align with our observation that ILPR variants forming stable i-motifs, such as ILPR 1_{mut}, are more transcriptionally active than those forming weaker or unstable structures. Together, this reinforces the emerging role of i-motifs as tuneable, responsive DNA elements capable of regulating gene expression in a glucose-sensitive manner.

G-quadruplexes and i-motifs are noncanonical DNA structures that can form within genomic DNA, yet their presence is temporally regulated throughout the cell cycle, indicating distinct functional roles. Immunofluorescence studies using structure-specific antibodies showed that G-quadruplexes tend to form during S-phase when DNA is unwound for replication, capable of stalling polymerases and influencing transcription and replication timing [22]. Conversely, i-motifs, which form on the complementary C-rich strand, are predominantly observed during late G1 to early S-phase [22], although stable i-motifs have been indicated to cause mutations in some examples [76], overall this suggests a more dynamic and regulatory role. The formation of the G-quadruplex and i-motif within the 2.5 repeating units of ILPR in the reporter system studied here has been indicated to be mutually exclusive, likely due to the greater thermodynamic and mechanical stability of the G-quadruplex under G-quadruplex stabilising conditions [26, 77]. However, this does not preclude the possibility that the complementary C-rich strand remains unpaired thereby making i-motif formation plausible under certain conditions such as transient decreases in pH during cellular metabolism. Nonetheless, these noncanonical structures may act in concert by providing binding sites for regulatory proteins. Early work suggested that Pur-1/MAZ could interact with the ILPR, however the absence of DNA-only controls in this work complicates the distinguishment between protein-DNA complexes from higher-order DNA multimers [8]. Other evidence has been reported for insulin and insulin-like growth factor 2 (IGF-2), which have been shown to bind the ILPR G-quadruplexes selectively both *in vitro* and within chromatin

[12, 46, 78]. Although early foot printing experiments did not clearly demonstrate i-motif formation in the C-rich [26, 79] strand our previous work using CD, NMR and solving the X-ray crystal structure indicated the C-rich sequence forms an intramolecular i-motif structure [25]. Taken together, the dynamic and context-dependent nature of both G-quadruplex and i-motif formation suggests a potential finely tuned regulatory mechanism sensitive to the cellular environment. This aligns with the observation that pancreatic β-cells possess a tightly controlled and protected cell cycle, with limited responsiveness to proliferative stimuli to preserve their differentiated state and insulin-secreting function [80]. These constraints reinforce the need for highly regulated transcriptional programs to maintain glucose homeostasis and support a model in which dynamic noncanonical DNA structures like those within the ILPR contribute to fine-tuned gene regulation in β-cells. Zeraati *et al.* demonstrated the presence of i-motifs in human nuclei with peak formation in late G1 phase, implying that i-motifs respond to finely tuned cellular cues, such as pH or redox state [22, 81]. Further evidence underscores this regulatory significance by showing that it is the stability of i-motifs, rather than G-quadruplexes, that correlates with spontaneous deletion events in human cells [76]. These deletions were more frequent at loci with stable i-motifs, suggesting that the persistence of i-motif structures may interfere with genomic processes such as repair or replication. Collectively, these findings support a model in which G-quadruplexes may serve as a region to initiation transcription, while i-motifs act as tuneable regulator, with the potential to regulate insulin gene expression and possibly impact genome stability.

Conclusions

In summary, our findings support a model in which noncanonical DNA structures within the ILPR may contribute to the regulation of insulin gene expression by providing potential binding sites for regulatory proteins. It will be interesting to see whether this is also true for other promoter regions in the genome. Indeed, emerging evidence suggests that G-quadruplexes and i-motifs formed in different promotor regions can play distinct and context-dependent roles at different genomic loci and chromatin environment. The current working hypothesis is, in case of the ILPR, the G-quadruplex may act as an initiation site that enables or restrict transcription, while the i-motif functions as modulator that fine-tune transcription output. This work further emphasizes the importance of considering G-quadruplex and i-motif DNA structures as one dynamic regulatory system with implications for both the insulin gene regulation and for exploring i-motifs and G-quadruplexes as potential therapeutic targets in diabetes.

Acknowledgements

Author contributions: Z.A.E.W., Y.D., S.S.S., and T.D.C. secured the research funding, conceived and designed the study. D.G. designed, performed, and analysed the biophysical and cell-based studies. D.G. and Z.A.E.W. wrote the first draft of the paper. D.G., C.J.M., Y.D., T.D.S., S.S.S., and Z.A.E.W. contributed to the review and editing of the manuscript.

Supplementary data

Supplementary data is available at NAR online.

Conflict of interest

None declared.

Funding

United Kingdom Biotechnology and Biological Sciences Research Council (BBSRC) [BB/W000962/1 to D.G., Z.A.E.W., Y.D., and T.D.C.].

Data availability

All data is available on Zenodo DOI:10.5281/zenodo.15320278.

References

1. Bennett ST, Todd JA. Human type 1 diabetes and the insulin gene: principles of mapping polygenes. *Annu Rev Genet* 1996;30:343–70.
2. Bell GI, Horita S, Karam JH. A polymorphic locus near the human insulin gene is associated with insulin-dependent diabetes mellitus. *Diabetes* 1984;33:176–83. https://doi.org/10.2337/diab.33.2.176
3. Bell GI, Pictet RL, Rutter WJ *et al.* Sequence of the human insulin gene. *Nature* 1980;284:26–32. https://doi.org/10.1038/284026a0
4. Bell GI, Selby MJ, Rutter WJ. The highly polymorphic region near the human insulin gene is composed of simple tandemly repeating sequences. *Nature* 1982;295:31–5. https://doi.org/10.1038/295031a0
5. Rotwein PS, Chirgwin J, Province M *et al.* Polymorphism in the 5′ flanking region of the human insulin gene: a genetic marker for non-insulin-dependent diabetes. *N Engl J Med* 1983;308:65–71. https://doi.org/10.1056/NEJM198301133080202
6. Hammond-Kosack MC, Dobrinski B, Lurz R *et al.* The human insulin gene linked polymorphic region exhibits an altered DNA structure. *Nucleic Acids Res* 1992;20:231–6. https://doi.org/10.1093/nar/20.2.231
7. Kennedy GC, German MS, Rutter WJ. The minizatellite in the diabetes susceptibility locus IDDM2 regulates insulin transcription. *Nat Genet* 1995;9:293–8. https://doi.org/10.1038/ng0395-293
8. Lew A. Unusual DNA structure of the diabetes susceptibilitylocus IDDM2 and its effect on transcription by theinsulin promoter factor pur-1/MAZ. *Proc Natl Acad Sci USA* 2000;97:12508–12. https://doi.org/10.1073/pnas.97.23.12508
9. DeFronzo RA, Ferrannini E, Groop L *et al.* Type 2 diabetes mellitus. *Nat Rev Dis Primers* 2015;1:15019. https://doi.org/10.1038/nrdp.2015.19
10. Miranda MA, Macias-Velasco JF, Lawson HA. Pancreatic β-cell heterogeneity in health and diabetes: classes, sources, and subtypes. *Am J Physiol Endocrinol Metab* 2021;320:E716–31. https://doi.org/10.1152/ajpendo.00649.2020
11. Rotwein P, Yokoyama S, Didier DK *et al.* Genetic analysis of the hypervariable region flanking the human insulin gene. *Am J Hum Genet* 1986;39:291–9.
12. Xiao J, Carter JA, Frederick KA *et al.* A genome-inspired DNA ligand for the affinity capture of insulin and insulin-like growth factor-2. *J Sep Sci* 2009;32:1654–64. https://doi.org/10.1002/jssc.200900060
13. Gehring K, Leroy J-L, Guéron M. A tetrameric DNA structure with protonated cytosine-cytosine base pairs. *Nature* 1993;363:561–5. https://doi.org/10.1038/363561a0
14. Catasti P, Chen X, Deaven LL *et al.* Cytosine-rich strands of the insulin minizatellite adopt hairpins with intercalated cytosine+.cytosine pairs. *J Mol Biol* 1997;272:369–82. https://doi.org/10.1006/jmbi.1997.1248

15. Dhakal S, Lafontaine JL, Yu Z *et al.* Intramolecular folding in human ILPR fragment with three C-rich repeats. *PLoS One* 2012;7:e39271. https://doi.org/10.1371/journal.pone.0039271
16. Zhou J, Wei C, Jia G *et al.* Formation of i-motif structure at neutral and slightly alkaline pH. *Mol Biosyst* 2010;6:580–6. https://doi.org/10.1039/B919600E
17. Rajendran A, S-i Nakano, Sugimoto N. Molecular crowding of the cosolutes induces an intramolecular i-motif structure of triplet repeat DNA oligomers at neutral pH. *Chem Commun* 2010;46:1299–301. https://doi.org/10.1039/b922050j
18. Hardin CC, Watson T, Corregan M *et al.* Cation-dependent transition between the quadruplex and Watson-Crick hairpin forms of d(CGCG3GCG). *Biochemistry* 1992;31:833–41. https://doi.org/10.1021/bi00118a028
19. Sekibo DAT, Fox KR. The effects of DNA supercoiling on G-quadruplex formation. *Nucleic Acids Res* 2017;45:12069–79. https://doi.org/10.1093/nar/gkx856
20. Sun D, Hurley LH. The importance of negative superhelicity in inducing the formation of G-quadruplex and i-motif structures in the c-myc promoter: implications for drug targeting and control of gene expression. *J Med Chem* 2009;52:2863–74. https://doi.org/10.1021/jm900055s
21. Dzatko S, Krafcikova M, Hansel-Hertsch R *et al.* Evaluation of the stability of DNA i-motifs in the nuclei of living mammalian cells. *Angew Chem Int Ed Engl* 2018;57:2165–9. https://doi.org/10.1002/anie.201712284
22. King JJ, Irving KL, Evans CW *et al.* DNA G-quadruplex and i-motif structure formation is interdependent in Human cells. *J Am Chem Soc* 2020;142:20600–4. https://doi.org/10.1021/jacs.0c11708
23. Zanin I, Ruggiero E, Nicoletto G *et al.* Genome-wide mapping of i-motifs reveals their association with transcription regulation in live human cells. *Nucleic Acids Res* 2023;51:8309–21. https://doi.org/10.1093/nar/gkad626
24. Víšková P, Ištvánková E, Ryneš J *et al.* In-cell NMR suggests that DNA i-motif levels are strongly depleted in living human cells. *Nat Commun* 2024;15:1992.
25. Guneri D, Alexandrou E, El Omari K *et al.* Structural insights into i-motif DNA structures in sequences from the insulin-linked polymorphic region. *Nat Commun* 2024;15:7119. https://doi.org/10.1038/s41467-024-50553-0
26. Dhakal S, Yu Z, Konik R *et al.* G-quadruplex and i-motif are mutually exclusive in ILPR double-stranded DNA. *Biophys J* 2012;102:2575–84. https://doi.org/10.1016/j.bpj.2012.04.024
27. Mergny JL, Lacroix L. UV melting of G-quadruplexes. *Curr Protoc Nucleic Acid Chem* 2009;Chapter 17:17.1.1–17.1.15.
28. Baker JM, Boyce FM. High-throughput functional screening using a homemade dual-glow luciferase assay. *J Vis Exp* 2014;88:e50282. https://doi.org/10.3791/50282-v
29. Yang B, Guneri D, Yu H *et al.* Prediction of DNA i-motifs via machine learning. *Nucleic Acids Res* 2024;52:2188–97. https://doi.org/10.1093/nar/gkae092
30. Choi J, Kim S, Tachikawa T *et al.* pH-induced intramolecular folding dynamics of i-motif DNA. *J Am Chem Soc* 2011;133:16146–53. https://doi.org/10.1021/ja2061984
31. Day HA, Pavlou P, Waller ZAE. i-motif DNA: structure, stability and targeting with ligands. *Bioorg Med Chem* 2014;22:4407–18. https://doi.org/10.1016/j.bmc.2014.05.047
32. Yazdani K, Seshadri S, Tillo D *et al.* Decoding complexity in biomolecular recognition of DNA i-motifs with microarrays. *Nucleic Acids Res* 2023;51:12020–30. https://doi.org/10.1093/nar/gkad981
33. Phan AT, Guéron M, Leroy J-L. The solution structure and internal motions of a fragment of the cytidine-rich strand of the human telomere11Edited by I. Tinoco. *J Mol Biol* 2000;299:123–44. https://doi.org/10.1006/jmbi.2000.3613
34. Benabou S, Garavís M, Lyonnais S *et al.* Understanding the effect of the nature of the nucleobase in the loops on the stability of the i-motif structure. *Phys Chem Chem Phys* 2016;18:7997–8004. https://doi.org/10.1039/C5CP07428B
35. Školáková P, Renčiuk D, Palacký J *et al.* Systematic investigation of sequence requirements for DNA i-motif formation. *Nucleic Acids Res* 2019;47:2177–89.
36. Li H, Hai J, Zhou J *et al.* The formation and characteristics of the i-motif structure within the promoter of the c-myb proto-oncogene. *J Photochem Photobiol B* 2016;162:625–32. https://doi.org/10.1016/j.jphotobiol.2016.07.035
37. Iaccarino N, Cheng M, Qiu D *et al.* Effects of sequence and base composition on the CD and TDS profiles of i-DNA. *Angew Chem Int Ed Engl* 2021;60:10295–303. https://doi.org/10.1002/anie.202016822
38. Day HA, Wright EP, MacDonald CJ *et al.* Reversible DNA i-motif to hairpin switching induced by copper(ii) cations. *Chem Commun* 2015;51:14099–102. https://doi.org/10.1039/C5CC05111H
39. Kendrick S, Kang HJ, Alam MP *et al.* The dynamic character of the BCL2 promoter i-motif provides a mechanism for modulation of gene expression by compounds that bind selectively to the alternative DNA hairpin structure. *J Am Chem Soc* 2014;136:4161–71. https://doi.org/10.1021/ja410934b
40. Lieblein AL, Fürtig B, Schwalbe H. Optimizing the kinetics and thermodynamics of DNA i-motif folding. *ChemBioChem* 2013;14:1226–30. https://doi.org/10.1002/cbic.201300284
41. Mergny JL, Li J, Lacroix L *et al.* Thermal difference spectra: a specific signature for nucleic acid structures. *Nucleic Acids Res* 2005;33:e138. https://doi.org/10.1093/nar/gni134
42. Mergny J-L, Lacroix L. Analysis of thermal melting curves. *Oligonucleotides* 2003;13:515–37. https://doi.org/10.1089/154545703322860825
43. Catasti P, Chen X, Moyzis RK *et al.* Structure-function correlations of the insulin-linked polymorphic region. *J Mol Biol* 1996;264:534–45. https://doi.org/10.1006/jmbi.1996.0659
44. Yu Z, Schonhoft JD, Dhakal S *et al.* ILPR G-quadruplexes formed in seconds demonstrate high mechanical stabilities. *J Am Chem Soc* 2009;131:1876–82. https://doi.org/10.1021/ja806782s
45. Schonhoft JD, Bajracharya R, Dhakal S *et al.* Direct experimental evidence for quadruplex–quadruplex interaction within the human ILPR. *Nucleic Acids Res* 2009;37:3310–20. https://doi.org/10.1093/nar/gkp181
46. Xiao J, McGown LB. Mass spectrometric determination of ILPR G-quadruplex binding sites in insulin and IGF-2. *J Am Soc Mass Spectrom* 2009;20:1974–82. https://doi.org/10.1016/j.jasms.2009.08.002
47. Schonhoft JD, Das A, Achamyeleh F *et al.* ILPR repeats adopt diverse G-quadruplex conformations that determine insulin binding. *Biopolymers* 2010;93:21–31. https://doi.org/10.1002/bip.21289
48. Kikin O, D'Antonio L, Bagga PS. QGRS Mapper: a web-based server for predicting G-quadruplexes in nucleotide sequences. *Nucleic Acids Res* 2006;34:W676–82. https://doi.org/10.1093/nar/gkl253
49. Stiernet P, Nenquin M, Moulin P *et al.* Glucose-induced cytosolic pH changes in beta-cells and insulin secretion are not causally related: studies in islets lacking the Na+/H+ exchangeR NHE1. *J Biol Chem* 2007;282:24538–46. https://doi.org/10.1074/jbc.M702862200
50. Thompson B, Satin LS. Beta-cell ion channels and their role in regulating insulin secretion. *Comprehensive Physiology* 2021;11:1–21. https://doi.org/10.1002/j.2040-4603.2021.tb00189.x
51. Rajas F, Gautier-Stein A, Mithieux G. Glucose-6 phosphate, a central hub for liver carbohydrate metabolism. *Metabolites* 2019;9:282. https://doi.org/10.3390/metabo9120282
52. Tanaka R, Sugiura K, Osabe K *et al.* Genetically encoded bioluminescent glucose indicator for biological research. *Biochem Biophys Res Commun* 2025;742:151092. https://doi.org/10.1016/j.bbrc.2024.151092

53. Spencer NY, Yan Z, Boudreau RL *et al.* Control of hepatic nuclear superoxide production by glucose 6-phosphate dehydrogenase and NADPH oxidase-4. *J Biol Chem* 2011;286:8977–87. https://doi.org/10.1074/jbc.M110.193821
54. Sun RC, Dukhande VV, Zhou Z *et al.* Nuclear glycogenolysis modulates histone acetylation in Human non-small cell lung cancers. *Cell Metab* 2019;30:903–16. https://doi.org/10.1016/j.cmet.2019.08.014
55. Sutendra G, Kinnaird A, Dromparis P *et al.* A nuclear pyruvate dehydrogenase complex is important for the generation of acetyl-CoA and histone acetylation. *Cell* 2014;158:84–97. https://doi.org/10.1016/j.cell.2014.04.046
56. Lorenz MA, El Azzouny MA, Kennedy RT *et al.* Metabolome response to glucose in the β-cell line INS-1 832/13. *J Biol Chem* 2013;288:10923–35. https://doi.org/10.1074/jbc.M112.414961
57. Neupane A, Chariker JH, Rouchka EC. Analysis of nucleotide variations in human G-quadruplex forming regions associated with dizease states. *Genes (Basel)* 2023;14. https://doi.org/10.3390/genes14122125
58. Chen Y, Long J, Wu S *et al.* Disruption of a DNA G-quadruplex causes a gain-of-function SCL45A1 variant relevant to developmental disorders. *Acta Biochim Biophys Sin (Shanghai)* 2024;56:709–16. https://doi.org/10.3724/abbs.2024053
59. Siddiqui-Jain A, Grand CL, Bearss DJ *et al.* Direct evidence for a G-quadruplex in a promoter region and its targeting with a small molecule to repress c-MYC transcription. *Proc Natl Acad Sci USA* 2002;99:11593–8. https://doi.org/10.1073/pnas.182256799
60. Matschinsky FM, Ellerman JE. Metabolism of glucose in the islets of Langerhans. *J Biol Chem* 1968;243:2730–6. https://doi.org/10.1016/S0021-9258(18)93432-0
61. Docherty HM, Hay CW, Ferguson LA *et al.* Relative contribution of PDX-1, MafA and E47/beta2 to the regulation of the human insulin promoter. *Biochem J* 2005;389:813–20. https://doi.org/10.1042/BJ20041891
62. Gray JP, Alavian KN, Jonas EA. Heart EA: NAD kinase regulates the size of the NADPH pool and insulin secretion in pancreatic beta-cells. *Am J Physiol Endocrinol Metab* 2012;303:E191–199. https://doi.org/10.1152/ajpendo.00465.2011
63. Kuroda A, Rauch TA, Todorov I *et al.* Insulin gene expression is regulated by DNA methylation. *PLoS One* 2009;4:e6953. https://doi.org/10.1371/journal.pone.0006953
64. Ye Y, Barghouth M, Dou H *et al.* A critical role of the mechanosensor PIEZO1 in glucose-induced insulin secretion in pancreatic beta-cells. *Nat Commun* 2022;13:4237. https://doi.org/10.1038/s41467-022-31103-y
65. Cottet-Dumoulin D, Lavallard V, Lebreton F *et al.* Biosynthetic activity differs between islet cell types and in beta cells is modulated by glucose and not by secretion. *Endocrinology* 2021;162:1–11. https://doi.org/10.1210/endocr/bqaa239
66. Kim H-Y. Statistical notes for clinical researchers: chi-squared test and Fisher's exact test. *Restor Dent Endod* 2017;42:152–5. https://doi.org/10.5395/rde.2017.42.2.152
67. Schober P, Boer C, Schwarte LA. Correlation coefficients: appropriate use and interpretation. *Anesth Analg* 2018;126:1763–68. https://doi.org/10.1213/ANE.0000000000002864
68. Wright EP, Lamparska K, Smith SS *et al.* Substitution of cytosine with guanylurea decreases the stability of i-motif DNA. *Biochemistry* 2017;56:4879–83. https://doi.org/10.1021/acs.biochem.7b00628
69. Mir B, Solés X, González C *et al.* The effect of the neutral cytidine protonated analogue pseudoisocytidine on the stability of i-motif structures. *Sci Rep* 2017;7:2772. https://doi.org/10.1038/s41598-017-02723-y
70. Stadlbauer P, Kührová P, Banáš P *et al.* Hairpins participating in folding of human telomeric sequence quadruplexes studied by standard and T-REMD simulations. *Nucleic Acids Res* 2015;43:9626–44.
71. Zhang Z-H, Qian SH, Wei D *et al. In vivo* dynamics and regulation of DNA G-quadruplex structures in mammals. *Cell Biosci* 2023;13:117. https://doi.org/10.1186/s13578-023-01074-8
72. Dai J, Dexheimer TS, Chen D *et al.* An intramolecular G-quadruplex structure with mixed parallel/antiparallel G-strands formed in the human BCL-2 promoter region in solution. *J Am Chem Soc* 2006;128:1096–8. https://doi.org/10.1021/ja055636a
73. González V, Guo K, Hurley L *et al.* Identification and characterization of Nucleolin as a c-myc G-quadruplex-binding protein. *J Biol Chem* 2009;284:23622–35. https://doi.org/10.1074/jbc.M109.018028
74. Wright EP, Huppert JL, Waller ZAE. Identification of multiple genomic DNA sequences which form i-motif structures at neutral pH. *Nucleic Acids Res* 2017;45:2951–9. https://doi.org/10.1093/nar/gkx090
75. Kaiser CE, Van Ert NA, Agrawal P *et al.* Insight into the complexity of the i-motif and G-quadruplex DNA structures formed in the KRAS promoter and subsequent drug-induced gene repression. *J Am Chem Soc* 2017;139:8522–36. https://doi.org/10.1021/jacs.7b02046
76. Martella M, Pichiorri F, Chikhale RV *et al.* Smith SS: i-motif formation and spontaneous deletions in human cells. *Nucleic Acids Res* 2022;50:3445–55. https://doi.org/10.1093/nar/gkac158
77. Cui Y, Kong D, Ghimire C *et al.* Mutually exclusive formation of G-quadruplex and i-motif is a general phenomenon governed by steric hindrance in duplex DNA. *Biochemistry* 2016;55:2291–9. https://doi.org/10.1021/acs.biochem.6b00016
78. Wang Y, Zhang H, Ligon LA *et al.* Association of insulin-like growth factor 2 with the insulin-linked polymorphic region in cultured fetal thymus cells. *Biochemistry* 2009;48:8189–94. https://doi.org/10.1021/bi900958x
79. Dhakal S, Schonhoft JD, Koirala D *et al.* Coexistence of an ILPR i-motif and a partially folded structure with comparable mechanical stability revealed at the single-molecule level. *J Am Chem Soc* 2010;132:8991–7. https://doi.org/10.1021/ja100944j
80. Szabat M, Lynn FC, Hoffman BG *et al.* Maintenance of β-cell maturity and plasticity in the adult pancreas: developmental biology concepts in adult physiology. *Diabetes* 2012;61:1365–71. https://doi.org/10.2337/db11-1361
81. Abdelhamid MA, Fabian L, MacDonald CJ *et al.* Redox-dependent control of i-motif DNA structure using copper cations. *Nucleic Acids Res* 2018;46:5886–93. https://doi.org/10.1093/nar/gky390

Received: May 2, 2025. **Revised:** December 6, 2025. **Accepted:** December 28, 2025